Research Article

Mitigation of Sub-Synchronous Resonance with Static Synchronous Series Compensator

Nilaykumar A Patel[1,*], Praghnesh J Bhatt[2]

[1, 2] Chnadubhai S. Patel Institute of Technology, Charotar University of Science and Technology, Changa, India

Received: 03/05/2017
Revised: 22/06/2017
Accepted: 27/06/2017

Correspondence to:
*Nilaykumar A. Patel:
nilaypatel.cem@charusat.ac.in:

Abstract:

The rapid growth of power sector and emergence to bulk power transfer over long transmission line demand series compensation to ensuring stable operation of power system. The series compensation of transmission line by fixed series capacitors may potentially lead to subsynchronous-resonance (SSR) issues. This paper presents the detailed modeling of different power system components which play an instrumental role in SSR phenomena. IEEE first benchmark model (FBM) is used to simulate SSR phenomena and eigenvalue analysis has been presented to identify potential modes that can lead to SSR. The modeling of Static Synchronous Series Capacitors (SSSC) is presented to mitigate SSR. The coordination of automatic voltage regulator (AVR) and power system stabilizer (PSS) are explored to mitigate in accordance with SSSC.

Keywords: Eigenvalues, IEEEFBM, SSR, Series Compensation, SSSC

I. INTRODUCTION

In subsynchronous resonance (SSR), the electric network exchanges the energy with a turbine generator at one or more of the natural frequencies of the combinedsystem below the synchronous frequency of the system [1]-[2]. The SSR phenomenon had first reported at the Mohave power plant in United States of America where incidences of two successive shaft failures occurred in 1970 and 1971. The extensive researches have been started then after to understand the SSR phenomenon and the researchers have came up with the countermeasures to mitigate the SSR phenomenon by increasing the damping capability of the electrical power system.The series compensation of the transmission lines have been utilized for the long transmission line in order to enhance power transfer capability and stability of power system, but on the other hand it gives rise to undesirable SSR oscillations [3]. There are two main characteristic of SSR phenomenon, namely, (a) self-excitation (also known as steady state SSR) and (b) transient torques (also known as transient SSR) [4].

(a) Steady State SSR

The currents with sub-synchronous frequency entering into generator terminals produce sub-synchronous frequency terminal voltage components. These voltages can sustain sub-synchronous frequency currents to produce the effect that is termed as self-excitation. The self-excitation is divided into two categories: (i) Only rotor electrical dynamics is involved and termed as induction generator effect (IGE) and (ii) Both rotor electrical and mechanical dynamics are involved and termed as torsional interaction (TI).

IGE Effect

When the rotor runs faster than the rotating magneticfield produced by the sub-synchronous armature currents, the IGE effect can be observed. As a result, the rotor resistance turns to be negative as viewed from the armature terminals. When this negative rotor resistance becomes higher than the sum of armature and network resistances at a resonant frequency, self-excitation will be produced in synchronous generator which results in excessive voltages and currents.

TI Effect

When the sub-synchronous torque induced in the generator is electrically very close to one of the natural modes of the generator shaft, it can set up the conditions for the exchange of energy at a sub-synchronous frequency. Thus, it can cause the serious damage to the turbine-generator shaft.

(b) Transient SSR

The system disturbances such as sudden load changes, faults or tripping of the lines can excite oscillatory torques on the generator rotor. The setransient oscillatory electrical torques have many components such as unidirectional, exponentially decaying as well as oscillatory torques ranging from sub-synchronous to multiples of network frequency. The sub-synchronous frequency components of torque may have large amplitudes just after the disturbance and they may affect the shaft life due to fatigue damage.

The different methods for SSR analysis have been reported in literature. The methods based on Eigenvalue analysis for SSR analyses are outlined in [5–7] where as methods based on frequency scanning are reported in [8–10]. The methods based on the time domain simulation has been presented in [11] with Electromagnetic Transient Program (EMTP). For SSR studies, Eigenvalue analysis is an effective tool and can be used to verify the effects of system parameters on the SSR. Moreover, the evaluation of damping effects of different SSR modes can be possible and countermeasures of SSR mitigation can be designed [11]-[13]. In [14]-[16], studies on SSR with eigenvalue analysis have been presented. The requirement of construction of state equations from the dynamic model of network comprises of synchronous machine, turbine-generator masses, exciters and network are pointed out in [17]-[18] to carry out the eigenvalue analysis. In [18], proper tree of the network is obtained by complex topology analysis for state equations construction.

II. POWER SYSTEM MODELLING OF SSR STUDIES

The eigenvalue analysis is adopted in this work for SSR studies. The state space equation of dynamic system including synchronous generator along with turbine stages, excitation system and the electric network with SSSC have been formulated. The formulation of state equation starts with individual component modelling which subsequently integrated to form overall combined state space equations for the computation of eigenvalues of entire network.

A. Modelling of Synchronous Machine

Type 2.2 model of synchronous machine is used in this work which has two windings on d- and q- axis of the rotor. The model of the synchronous machine has three damper coils to capture accurate dynamics of the machine. Three phase armature winding on the stator (a, b and c phase), one field winding (fd) in d-axis of rotor along with the damper windings (g) and two damper windings (h and k) on q-axis of the rotor are considered [12]. Fig. 1 shows the rotor model of synchronous machine along with different masses of turbine as per the IEEE FBM model.

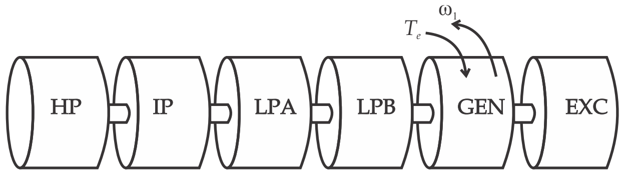

Fig. 1 Rotor Model from IEEE FBM

The state space equations for synchronous generator is given in (1).

$$\frac{d}{dt}\Delta x_e = [A_e]\Delta x_e + [B_{eN}]\begin{bmatrix}\Delta V_{qs} \\ \Delta V_{ds}\end{bmatrix} + [B_{eM}]\Delta\omega + [B_{eP}]\begin{bmatrix}\Delta V_{kq1} \\ \Delta V_{kq2} \\ \Delta e_{xfd} \\ \Delta V_{kd}\end{bmatrix} \quad (1)$$

where

$$\Delta x_e^T = \begin{bmatrix}\Delta\psi_{qs} & \Delta\psi_{ds} & \Delta\psi_{kq1} & \Delta\psi_{kq2} & \Delta\psi_{fd} & \Delta\psi_{kd}\end{bmatrix}$$

B. Modelling of Turbine-Generator Unit – Mechanical System

The turbine–generator unit considered as lumped masses forms the mechanical system and it consists of six masses of different pressure stages as shown in Fig. 1. The synchronous generator and an exciter are also coupled on the same shaft. The state equation for mechanical system is given in (2).

$$\frac{d}{dt}\Delta x_m = [A_m]\Delta x_m + [B_{mN}][\Delta T_m] + [B_{mM}][B_{EE}]\Delta x_e \quad (2)$$

where

$$\Delta x_m^T = \begin{bmatrix}\Delta\omega_E \ \Delta\omega_1 \ \Delta\omega_2 \ \Delta\omega_3 \ \Delta\omega_4 \ \Delta\omega_5 \\ \Delta\delta_E \ \Delta\delta_1 \ \Delta\delta_2 \ \Delta\delta_3 \ \Delta\delta_4 \ \Delta\delta_5\end{bmatrix}$$

C. Electrical Network

The electrical equivalent circuit for the IEEE first benchmark model to study SSR is shown in Fig. 2. The generator with constant voltage source Eg is connected to infinite bus through series compensated transmission line.

The state equations of electrical network in D–Q components are given in (3)

$$\frac{d}{dt}\Delta x_N = [A_N]\Delta x_N + [B_{Ne}][B_{ee}]\Delta x_e + [B_{Nm}][I_\omega]\Delta x_m \quad (3)$$

where

$$\Delta x_N = \begin{bmatrix} \Delta V_{cq} & \Delta V_{cd} \end{bmatrix}^T$$

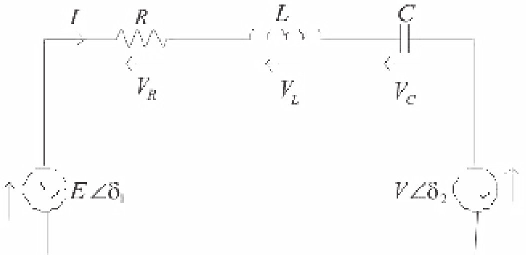

Fig. 2 Network Model of FBM

The voltage equations for the electrical network can be represented as (4).

$$\begin{bmatrix}\Delta e_q \\ \Delta e_d\end{bmatrix} = \underset{2X2}{[Z_L]}\underset{2X6}{[B_{ee}]}\underset{6X1}{\Delta x_e} + \underset{2X1}{\begin{bmatrix} \dfrac{X_L}{\omega_0} I_{d0} \\ -\dfrac{X_L}{\omega_0} I_{q0} \end{bmatrix}} \underset{1X12}{[I_\omega]}\underset{12X1}{\Delta x_m}$$

$$+\frac{X_L}{\omega_0}\underset{2X6}{[B_{ee}]}\frac{d}{dt}\underset{6X1}{\Delta x_e} + \underset{2X1}{\Delta x_N} + \underset{2X1}{\begin{bmatrix} -V_\infty \sin\delta_0 \\ V_\infty \cos\delta_0 \end{bmatrix}} \underset{1X12}{[I_\delta]}\underset{12X1}{\Delta x_m} \quad (4)$$

Integration of System Components

The individual model equations are required to integrate for the formulation of the state equations of overall system in order to capture the dynamic events. The state space equations for individual components given in (1)-(4) can be represented as (5). In (5), the dimensions of different matrices are clearly given for the better understanding of the overall state space equations.

III. SSSC MODELING FOR SSR MITIGATION

Static synchronous series compensator (SSSC) contains solid state controllable voltage source inverter which is connected in series with power transmission lines.

$$\frac{d}{dt}\underset{20X1}{\begin{bmatrix} \underset{6X1}{\Delta x_e} \\ \underset{12X1}{\Delta x_m} \\ \underset{2X1}{\Delta x_N} \end{bmatrix}} = \begin{bmatrix} \underset{6X6}{[A_E]} & \underset{5X12}{[B_{EM}]} & \underset{6X2}{[B_{EN}]} \\ \underset{12X6}{[B_{mM}][B_{EE}]} & \underset{12X12}{[A_m]} & \underset{12X2}{[0]} \\ \underset{2X6}{[B_{Ne}][B_{ee}]} & \underset{2X12}{[B_{Nm}][I_\omega]} & \underset{2X2}{[A_N]} \end{bmatrix} \underset{20X1}{\begin{bmatrix} \underset{6X1}{\Delta x_e} \\ \underset{12X1}{\Delta x_m} \\ \underset{2X1}{\Delta x_N} \end{bmatrix}} \quad (5)$$

$$+\begin{bmatrix} \underset{6X4}{B_{EP}} \\ \underset{14X4}{0} \end{bmatrix} \begin{bmatrix} \Delta V_{kq1} \\ \Delta V_{kq2} \\ \Delta e_{xfd} \\ \Delta V_{kd} \end{bmatrix} + \begin{bmatrix} \underset{6X4}{0} \\ \underset{12X4}{B_{mN}} \\ \underset{2X4}{0} \end{bmatrix} \underset{4X1}{[\Delta T_m]}$$

SSSC injects a controllable and sinusoidal voltage in series with the transmission network which can virtually change the reactance of line which in turn controls the transmission line power flow. This power flow control by SSSC is independent of the magnitude of the line current. The schematic of SSSC in series with transmission line is shown in Fig. 3. SSSC injects V_{ia} voltage in series with transmission line voltage, which can be control for control of power flow in the transmission line by controlling the modulation index (m) and phase angle θ_f.

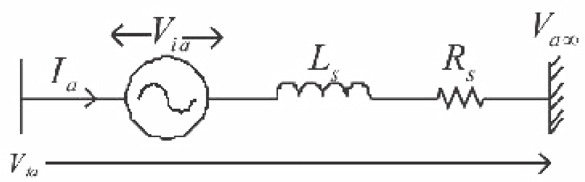

Fig. 3 SSSC connected transmission line

The injected voltage by SSSC is $V_{ia} = \frac{mV_{dc}}{2}\cos(\omega t + \theta_f)$ where value of m controls both the interfacing transformer ratio and modulation index. From Fig. 3, the sending end voltage of transmission line is written as

$$V_{ta} = V_{ia} + R_s i_a + L_s \frac{di_a}{dt} + V_{a\infty} \quad (6)$$

The SSSC compensated transmission line in d-q reference frame is derived as under and given in (7).

$$\begin{bmatrix} \frac{d}{dt} i_q \\ \frac{d}{dt} i_d \\ \frac{d}{dt} V_{dc} \end{bmatrix} = \begin{bmatrix} -\frac{\omega_b R_S}{X_S} & -\omega & -\frac{m\omega_b}{2X_S}\cos\theta_f \\ \omega & -\frac{\omega_b R_S}{X_S} & \frac{m\omega_b}{2X_S}\sin\theta_f \\ \frac{3m\omega_b X_{dc}}{4}\cos\theta_f & -\frac{3m\omega_b X_{dc}}{4}\sin\theta_f & -\frac{\omega_b X_{dc}}{R_{dc}} \end{bmatrix} \begin{bmatrix} i_q \\ i_d \\ V_{dc} \end{bmatrix} + \begin{bmatrix} \frac{\omega_b}{X_S} & 0 \\ 0 & \frac{\omega_b}{X_S} \\ 0 & 0 \end{bmatrix} \begin{bmatrix} V_{tq} \\ V_{td} \end{bmatrix} \quad (7)$$

A. Control of SSSC

The block diagram of SSSC control for SSR mitigation is shown in Fig. 4 and its state space modeling is given herewith.

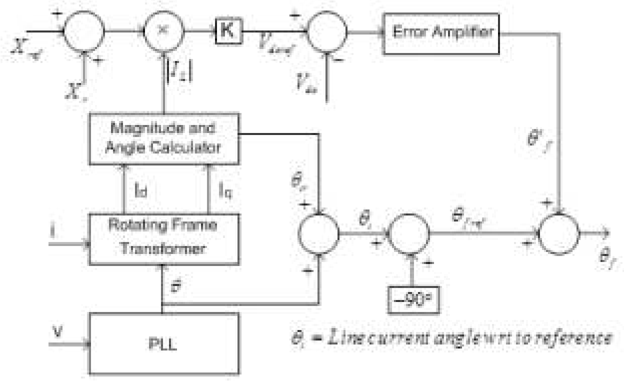

Fig. 4 Control of SSSC for SSR Mitigation

The dynamic equation of SSSC compensated network is as under.

$$\theta_f = \left(K_p + \frac{K_i}{S}\right)\left(V_{dc\,ref} - V_{dc}\right) + \theta_{f\,ref}$$

$$\frac{d}{dt}\Delta x_{SC} = \left[A_{SC}\right]\Delta x_{SC} + \left[A_{SCN}\right]\left[B_{ee}\right]\Delta x_e \qquad (8)$$

were

$$\Lambda x_{SC} = \left[\Lambda V_{dc} \quad \Lambda z\right] \qquad (9)$$

$$\left[A_{SC}\right] = \begin{bmatrix} -\dfrac{\omega_b X_{dc}}{R_{dc}} + \lambda K_p & -\lambda K_i \\ -1 & 0 \end{bmatrix} \qquad (10)$$

$$\left[A_{SCN}\right] = \begin{bmatrix} \alpha - \lambda K_p K' i_{q0} & -\beta - \lambda K_p K' i_{d0} \\ K' i_{q0} & K' i_{d0} \end{bmatrix} \qquad (11)$$

$$\alpha = \frac{3m\omega_b X_{dc}}{4}\cos\theta_{f0}\ , \quad \beta = \frac{3m\omega_b X_{dc}}{4}\sin\theta_{f0} \qquad (12)$$

$$and\ \lambda = \frac{3m\omega_b X_{dc}}{4}\left[i_{q0}\sin\theta_{f0} + i_{d0}\cos\theta_{f0}\right] \qquad (13)$$

and

$$\begin{bmatrix} \Delta V_q \\ \Delta V_d \end{bmatrix} = \frac{X_S}{\omega_b}\left[B_{ee}\right]\frac{d}{dt}\Delta x_e - \left[A_{SC1}\right]\left[B_{ee}\right]\Delta x_e + \left[B_{SC}\right]\left[I_{\omega\delta}\right]\Lambda x_m - \left[B_{SCDC}\right]\Lambda x_{SC}$$

The final equations of the overall system with SSSC control is given in (14)

$$\frac{d}{dt}\underset{20X1}{\begin{bmatrix} \underset{6X1}{\Delta x_e} \\ \underset{12X1}{\Delta x_m} \\ \underset{2X1}{\Delta x_{SC}} \end{bmatrix}} = \begin{bmatrix} \underset{6X6}{\left[A_{SCE}\right]} & \underset{6X12}{\left[B_{SCE}\right]} & \underset{6X2}{-\left[B_{ESC}\right]} \\ \underset{12X6}{\left[B_{mM}\right]\left[B_{EE}\right]} & \underset{12X12}{\left[A_m\right]} & \underset{12X2}{\left[0\right]} \\ \underset{2X6}{\left[A_{SCN}\right]\left[B_{ee}\right]} & \underset{2X12}{\left[0\right]} & \underset{2X2}{\left[A_{SC}\right]} \end{bmatrix} \underset{20X1}{\begin{bmatrix} \underset{6X1}{\Delta x_e} \\ \underset{12X1}{\Delta x_m} \\ \underset{2X1}{\Delta x_{SC}} \end{bmatrix}}$$

$$+ \begin{bmatrix} \underset{6X4}{B_{EP1}} \\ \underset{14X4}{0} \end{bmatrix} \begin{bmatrix} \Delta V_{kq1} \\ \Delta V_{kq2} \\ \Delta e_{xfd} \\ \Delta V_{kd} \end{bmatrix} + \begin{bmatrix} \underset{6X4}{0} \\ \underset{12X4}{B_{mN}} \\ \underset{2X4}{0} \end{bmatrix} \underset{4X1}{\left[\Delta T_m\right]} \qquad (14)$$

IV. MODELING OF AVR AND PSS

The use of AVR is needed for the synchronous generator to restore its terminal voltage automatically in the event of load changes or fault condition. To make response of AVR faster, the gain KA of PSS is set to higher value which in turn reduces the damping torque of the system. When the system is working at higher loading conditions and synchronous generator is connected to load through larger reactance, the use of AVR can result in negative damping torque in the system and the system may become oscillatory unstable. To avoid oscillatory instability and to compensate for negative damping torque effect of AVR, PSS as shown in Fig. 5 is used. PSS can provide the necessary phase shift through its lead-lag blocks depending on the requirement and can successfully make the system stable. The state equation with AVR+PSS on synchronous generator is given by (15).

V. RESULTS AND DISCUSSIONS

Fig. 5 Block Diagram of AVR and PSSThe state space equations for the system shown in Fig. 2 with fixed series compensation and SSSC are given in (5) and (14), respectively. Similarly, the state equation for the system including SSSC in transmission line and AVR-PSS at the synchronous generator is given in (15). The size of the state matrix for these three systems are (20 x 20), (20 x 20) and (25 x 25), respectively. The eigenvalues of these state matrices for these systems have been calculated and given in Table 1. The data for IEEE FBM shown in Fig. 2 are given in Appendix A. The series compensation level considered in this work is equal to 50% i.e. the total inductive reactance (including transformer and transmission line) is compensated by 50% by incorporating capacitive compensation. With the fixed series compensation of 50%, the eigenvalue analysis have been carried out for all three systems and reported in Table 1. In Table 1, the torsional modes have been identified which have the frequency of oscillations in sub-synchronous frequency range. Some torsional modes are highlighted which have the positive real part which is responsible to create subsynchronous resonance in the system. To stabilize these, torsional modes, SSSC has been adopted to provide series compensation instead

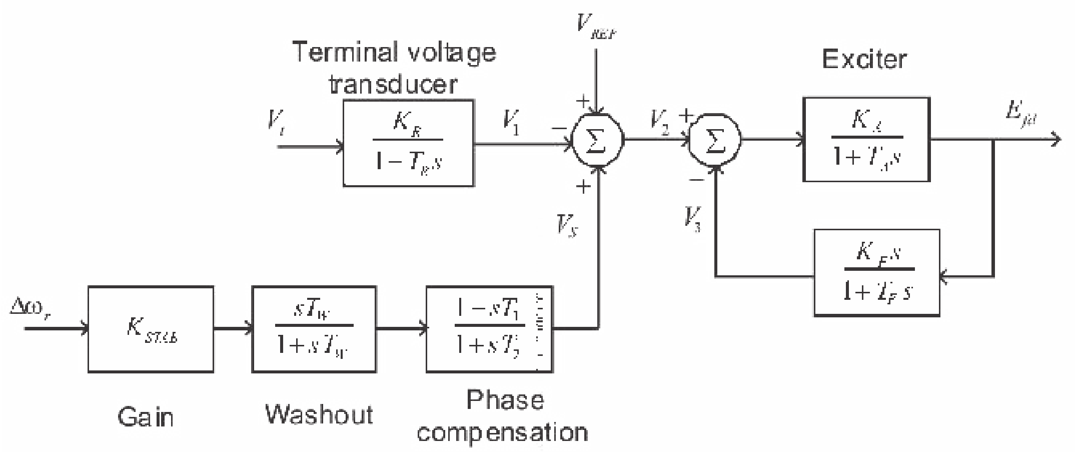

$$
\frac{d}{dt}\begin{bmatrix} \underset{6X1}{\Delta x_e} \\ \underset{12X1}{\Delta x_m} \\ \underset{2X1}{\Delta x_{sc}} \\ \underset{3X1}{\Delta x_{ex}} \\ \underset{2X1}{\Delta x_{pss}} \end{bmatrix}_{25X1} = \underbrace{\begin{bmatrix} \underset{6X6}{[A_{SCE}]} & \underset{6X12}{[B_{SCE}]} & \underset{6X2}{[B_{ESC}]} & \underset{6X3}{[B_{EX}]} & \underset{6X2}{0} \\ \underset{12X6}{[B_{mM}][B_{iF}]} & \underset{12X12}{[A_m]} & \underset{12X2}{0} & \underset{12X3}{0} & \underset{12X2}{0} \\ \underset{2X6}{[A_{SCN}][B_{ss}]} & \underset{2X12}{0} & \underset{2X2}{[A_{SC}]} & \underset{2X3}{0} & \underset{2X2}{0} \\ \underset{3X6}{[B_{exT}][A_{SCEF}]} & \underset{3X12}{[B_{exT}][B_{SCEF}]} & \underset{3X2}{[B_{exT}][B_{ESCF}]} & [A_{ex}]\ \underset{3X3}{[B_{exT}][B_{ENF}]} & \underset{3X2}{[B_{exT1}][I_{pss}]} \\ \underset{2X6}{0} & \underset{2X12}{[B_{pss}][I_\omega]} & \underset{2X2}{0} & \underset{2X3}{0} & \underset{2X3}{[A_{pss}]} \end{bmatrix}}_{25X25} \begin{bmatrix} \Delta x_e \\ \Delta x_m \\ \Delta x_{sc} \\ \Delta x_{ex} \\ \Delta x_{pss} \end{bmatrix}
$$

$$
+\begin{bmatrix} \underset{6X4}{0} \\ \underset{12X4}{[B_{mN}]} \\ \underset{7X4}{0} \end{bmatrix}[\Delta T_m] + \begin{bmatrix} \underset{6X3}{[B_{EP2}]} \\ \underset{14X3}{0} \\ \underset{3X3}{[B_{exT}][B_{EP2F}]} \\ \underset{2X3}{0} \end{bmatrix}\begin{bmatrix} \Delta V_{kq1} \\ \Delta V_{kq2} \\ \Delta V_{kd} \end{bmatrix} + \begin{bmatrix} \underset{21X1}{0} \\ \dfrac{K_F K_A}{T_F T_A} \\ \dfrac{K_A}{T_A} \\ \underset{2X1}{0} \end{bmatrix}\Delta v_{ref} \qquad (15)
$$

IEEE FBM with 50% series compensation	IEEE FBM 50% series compensation is replaced by SSSC	IEEE FBM SSSC+AVR-PSS	Modes of Oscillations
-4.716 ± 623.63i	-118.218 ± 547.17i	-84.56 ± 733.75i	Supersunchronous mode
-0.00000002 ± 297.97i	-0.181 ± 297.97i	-0.000002 ± 297.97i	Torsional mechanical mode
-0.00021 ± 202.84i	-0.025 ± 202.91i	-0.008 ± 202.88i	Torsional mechanical mode
-0.00036 ± 160.50i	-0.151 ± 160.53i	-0.0059 ± 160.51i	Torsional mechanical mode
0.0004 ± 126.94i	-0.65 ± 126.95i	-0.0022 ± 126.95i	Torsional mechanical mode
0.001 ± 98.70i	-0.016 ± 98.77i	-0.039 ± 98.71i	Torsional mechanical mode
-2.636 ± 130.35i	-10.00 ±47.06i	-3.89 ± 39.58i	Subsynchronous Mode
0.0013571638373	**1.179 ± 12.12i**	-0.001 ± 12.13i	Swing Mode
-0.0000000038616	-3.47 ± 0.77i	-0.64 ± 0.77i	Modes related to Damper and Field winding
-0.998 -4.4399 -20.467 -33.194	-20.509 -32.808	-2.763 ± 1.81i -20.470 -24.055 -35.690 -100.452 -494.272	

of fixed capacitors. In this case also, the torsional modes still persist but the use of SSSC can successfully damped the unstable torsional modes and the real part of all the eigenvalues related to torsional oscillations have turned to be negative, which is the indication that the system will not be unstable due to torsional oscillations. Thus, SSSC can be effective to mitigate the torsional oscillations but it leaves the system unstable with network modes which are highlighted in Table 1. In order to mitigate the SSR as well as to prevent the system to become unstable, the synchronous generator has been considered to have AVR and PSS. The eigenvalues with this case are also shown in Table 1 which show that the use of SSSC in transmission line and AVR-PSS at synchronous generator can successfully results in eigenvalues which have negative real part, thus it makes the system stable even with 50% of series compensation.

VI. CONCLUSION

The paper presents the state space modelling of different electrical components to study SSR of IEEE FBM. The series compensation of transmission network with certain degree of compensation may result in SSR. In this paper SSR phenomina is mitigated with the use of SSSC. The sub-synchronous, super-synchronous and torsional modes have been identified for IEEE FBM for 50% compensation. The torsional modes can be damped-out with the use of SSSC, but it leaves the system unstable by making eigenvalues positive corrosponding to swing mode. The use of PSS and AVR at synchronous generator in coordination with SSSC in transmission line can make the system stable and the torsional modes can be mitigated.

Appendix

Synchronous Machine Parameters for IEEE-FBM: Values are in pu

X_T=0.14 pu, R_L=0.02, X_L=0.50, X_{SYS}=0.06, X_C=0.371, P_g=0.9, V_T=1

Reactance	Value (pu)	Time Constant	Value (sec)
Xd	1.79	T'_{d0}	4.3
X'd	0.169	T''_{d0}	0.032
X”d	0.135	T'_{q0}	0.85
Xq	1.71	T''_{q0}	0.05
X'q	0.228		
X”q	0.2		
Xad	0.13		

Inertia	Inertia Constant (H)	Shaft section	Spring Constant (K) in pu torque/rad
HP turbine	0.092897	HP-IP	19.303
IP turbine	0.155589	IP-LPA	34.929
LPA turbine	0.85867	LPA-LPB	52.038
LPB turbine	0.884215	LPB-GEN	70.858
Generator	0.868495	GEN-EXC	2.82
Exciter	0.034217		

REFERENCES

[1] IEEE Subsynchronous Resonance Task Force. First benchmark model for computer simulation of subsynchronous resonance. IEEE Trans Power Apparatus System vol. 96, no. 5, pp. 1565–72, 1977

[2] IEEE SSR Working Group. Terms, definitions, and symbols for subsynchronous oscillations. IEEE Trans Power Apparatus System, vol. 104, no. 6, pp. 1326–33, 1985

[3] I.C. Report. Readers guide to subsynchronous resonance. IEEE Trans. Power System, vol. 7, no. 1, pp. 150–157.

[4] Kundur P. Power system stability and control. McGraw Hill; 1993.

[5] Framer RG, Katz E, Schwalb AL. Navajo project on subsynchronous resonance analysis and solutions. IEEE Trans PAS 1985:1057–66.

[6] Edris A. Series compensation schemes reducing the potential of resonance. IEEE Trans PAS 1990:219–26.

[7] Rana RD, Huff SW, Hayes RM, Fromholtz EN, Schulz RP. AEP's Kanawha river 345kV series capacitor installations-subsynchronous resonance studies and torsional measurements. In: Proceedings of the American power conference; 1991, p. 300–5.

[8] Zhu W, Spee R, Mohler RR, Alexander GG, Mittelstadt WA, Maratuhulam D. An EMTP study of SSR mitigation using the thyristor controlled series capacitor. IEEE Trans Power Delivery 1995; 10:1479–85.

[9] Dobson I, Chiang HD. Towards a theory of voltage collapse in electric power systems. Syst Cont lett 1989; 13:253–62.

[10] Ajjarapu A, Lee B. Bifurcation theory and its applications to nonlinear dynamical phenomena in an electrical power system. IEEE Trans Power Syst 1992; 7(1):424–31.

[11] Subsynchronous Resonance Working Group, Reader's guide to subsynchronous resonance, IEEE Transactions on Power Systems 7 (1) (1992) 150–157.

[12] R.Z. Davarani, R. Ghazi, N. Pariz, Nonlinear modal analysis of interaction between torsional modes and SVC controllers, Electric Power Systems Research91 (2012) 61–70.

[13] N. Kumar, M.P. Dave, Application of an auxiliary controlled static var system for damping subsynchronous resonance in power systems, Electric Power Systems Research 37 (3) (1996) 189–201.

[14] C. Gross, C.F. Imparato, P.M. Look, A tool for the comprehensive analysis of power system dynamic stability, IEEE Transactions on Power Apparatus and Systems 101 (1) (1982) 226–234.

[15] C. Yu, Z. Cai, Y. Ni, J. Zhong, Generalised eigenvalue and complex-torque-coefficient analysis for SSR study based on LDAE Model, IEE Proceedings-Generation, Transmission and Distribution 153 (1) (2006) 25–34.

[16] F.C. Jusan, S.G. Jr., G.N. Taranto, SSR results obtained with a dynamic phasor model of SVC using modal analysis, International Journal of Electrical Powerand Energy Systems 32 (6) (2010) 571–582.

[17] M. Parniani, M.R. Iravani, Computer analysis of small-signal stability of powersystems including network dynamics, IEE Proceedings-Generation, Transmis-sion and Distribution 142 (6) (1995) 613–617.

[18] P.M. Anderson, B.L. Agrawal, J.E. Vaness, Subsynchronous Resonance in Power Systems, Wiley-IEEE Press, New York, 1990.